

# MEASUREMENT OF TURBULENT FLOW IN A DUCT USING A TRACER GAS TECHNIQUE

## SUMMARY

We describe the use of the constant injection tracer gas technique to study turbulent flow in a rectangular duct. A comparison between tracer gas measurements and measurements made using a hot-wire anemometer and a pitot tube is presented. Measurement of tracer gas concentration, air velocity and pressure distribution at various distances from the duct wall and inlet were carried out. The Reynolds number based on the hydraulic diameter and the bulk velocity was varied between  $7.5 \times 10^4$  and  $18.6 \times 10^4$ . A theoretical expression for the entrance length required for fully developed turbulent flow was obtained and this was compared with experimental results.

S.B. Riffat, BSc, Dipl Tech, MSc, DPhil, MASHRAE, C Eng, MIMechE, MInst E

S.F. Lee, Dipl. Tech.

Department of Civil Engineering

Loughborough University of Technology,

Loughborough,

Leicestershire, LE11 3TU, UK

## LIST OF SYMBOLS

V	Internal volume of the duct ( $\text{m}^3$ )
C	Concentration of tracer gas (ppm)
$C_0$	Concentration of tracer gas at $t = 0$ (ppm)
C	Rate of change of concentration of tracer gas ( $\text{ppm s}^{-1}$ )
F	Volumetric flow rate ( $\text{m}^3 \text{s}^{-1}$ )
q	Injection flow rate of tracer gas ( $\text{m}^3 \text{s}^{-1}$ )
I	Air exchange rate ( $\text{h}^{-1}$ )
P	Pressure (Pa)
$h_a$	Atmospheric pressure (mm $\text{H}_2\text{O}$ )
$h_x$	Static pressure at point x along the duct (mm $\text{H}_2\text{O}$ )
U	Local time mean velocity ( $\text{m s}^{-1}$ )
$U_b$	Bulk velocity ( $\text{m s}^{-1}$ )
$U_m$	Maximum velocity in the fully developed region ( $\text{m s}^{-1}$ )
$U_c$	Centre line velocity ( $\text{m s}^{-1}$ )
$U_\tau$	Friction velocity ( $\text{m s}^{-1}$ )
g	Acceleration due to gravity ( $\text{m s}^{-2}$ )
$\rho$	Air density ( $\text{kg m}^{-3}$ )
$\rho_w$	Water density ( $\text{kg m}^{-3}$ )
$A_A$	Internal cross-sectional area of the bellmouth ( $\text{m}^2$ )
$A_B$	Internal cross-sectional area of the duct ( $\text{m}^2$ )
f	Friction factor
Z	Intercept of static pressure lines (mm $\text{H}_2\text{O}$ )
$\tau_w$	Wall shear stress (Pa)
Re	Reynolds number
$L_e$	Entrance length for fully developed flow (m)
$D_h$	Hydraulic diameter of the duct (m)

X	Distance from the duct inlet in the direction of flow (m)
y	Distance from the wall of the duct (mm)
t	Time (s)
H	Duct width (m)
W	Duct height (m)

## INTRODUCTION

The analysis of turbulent flow through ducts has considerable engineering importance in the design of fluid transporting systems such as HVAC systems, atomic power reactors, gas turbines and heat exchangers. Turbulent flow in ducts of various roughnesses, lengths and aspect ratios has been investigated previously using hot-wire anemometers, laser doppler velocimeters and pitot tubes<sup>(1-3)</sup>. The use of tracer gas techniques offers an alternative approach to work reported to date and offers the opportunity to develop improved air flow formulae. Tracer gas techniques have been widely used for measuring air flow in buildings<sup>(4-6)</sup> but only limited work has been published on the use of tracer gas techniques for the measurement of air flow in ducts<sup>(7-8)</sup>. There is a need to carry out a detailed study to determine the applicability of these techniques to the investigation of turbulent flow in ducts.

This paper describes the use of the constant injection tracer gas method for the estimation of air flow in a smooth duct. We have implemented this tracer gas technique to determine the entrance length,  $L_e$ , required for fully developed turbulent flow. Results derived from tracer gas measurements are compared with data obtained using a hot-wire anemometer and a pitot tube.

## FUNDAMENTALS OF THE CONSTANT INJECTION TRACER GAS TECHNIQUE

The constant injection tracer gas technique can be used to measure air flow in ducts. Assuming that the air and tracer gas are perfectly mixed within the duct and that the concentration of the tracer gas in the outside air is zero, the mass balance equation is:

$$V \frac{dC(t)}{dt} + F(t) C(t) = q(t) \quad (1)$$

The duct air exchange rate,  $I$ , is given by:

$$I(t) = F(t)/V \quad (2)$$

Assuming that the injection rate of tracer gas into the duct and that the duct air exchange rate are constant during the measurement, the solution of equation (1) is:

$$C(t) = q/F + (C_0 - q/F) \exp(-It) \quad (3)$$

If the system were close to equilibrium, the concentration of tracer gas would change slowly and the rate of change of concentration of tracer gas would be small. After a sufficiently long period, the transient term in equation (3) would die out and the flow rate through the duct would simply be given by:

$$C = q/F \quad (4)$$

Hence, if measurements of tracer gas flow rate and concentration can be made,  $F$  can be evaluated.

## EXPERIMENTAL APPARATUS AND INSTRUMENTATION

The duct shown in Figure 1 was constructed from 12mm thick plywood. The entrance to the duct consisted of a bellmouth made from wooden bars. The duct was 3m long and had an internal cross-section of 250mm x 40mm (i.e. the aspect ratio (W/H) of the duct was 6.25). The downstream end of the duct was connected to the suction side of a centrifugal fan by means of a diffuser. The flow rate of air through the duct was varied using a slide gate located at the discharge end of the fan. The centrifugal fan was driven by 335W AC motor.

Static and velocity pressure tapings were distributed at various positions ( $X/D_h = 4.1$  to 134) along the duct as shown in Figure 1. The velocity tapings allowed the insertion of a pitot tube or a hot wire anemometer. These could be traversed across the duct cross-section in order to measure velocity at various distances from the wall. A single tube inclined manometer, made by Air Flow Development Ltd, UK, was used to measure the static and velocity pressure heads.

The nitrous oxide tracer gas was injected at a constant rate into the duct inlet via a number of small injection tapings distributed around the perimeter of the duct. These tapings were connected to a manifold using flexible tubing. Nitrous oxide gas was supplied to the manifold via a type, F-100/200, mass flow controller which had maximum capability of 1 l/min and was manufactured by Bronkhorst High-Tech B V, Holland. The measurement accuracy of the mass flow controller was  $\pm 1\%$ . The flow rate was controlled using a variable power supply and the rate of tracer gas injection was displayed on a digital unit.

Tracer gas/air samples were collected using a sampling tube which could be positioned at various points along the length of the duct. This tube was mounted on a transversing mechanism which allowed samples to be taken at various distances from the duct wall. The air flow rate through the duct was estimated, using equation (4), by measuring the concentration of tracer gas in the air upstream from the fan.

The concentration of  $N_2O$  tracer gas was measured using an IRGA 120 Infra-red Gas Analyzer. The instrument, manufactured by J and S Sieger Ltd, UK, was a two beam gas analyzer equipped with a gas filled detector of the Luft type. The two beams of infra-red radiation of equal energy were interrupted at 6.6 Hz by a rotating shutter. These two series of pulses of infra-red energy passed simultaneously, one through an analysis cell, the other through a parallel reference cell, into a detector. The detector consisted of two sealed absorption chambers separated by a thin diaphragm. The absorption chambers were filled with a quantity of gas ( $N_2O$ ) for which the instrument was calibrated. The amount of infra-red absorption was measured and converted to parts-per-million (ppm) for a direct read-out on a meter.

## **THEORETICAL ANALYSIS OF TURBULENT FLOW IN A DUCT**

The formation of a boundary layer in a duct is shown in Figure 2. Air enters the duct at point "a" with a velocity  $U_a$ . At point "b" the velocity is uniform across the section of the duct. At point "f" the boundary layer is completely formed. Further downstream from point "f" the boundary layer has a constant thickness. Here the influence of the entrance shape upon the air flow pattern has disappeared and fully developed flow is said to exist.

We carried out measurements of tracer gas concentration and pressure distribution along the duct in order to determine an expression for the entrance length required for turbulent flow to be fully developed.

Considering Figure 2, and applying the continuity equation to sections A and B, we have:

$$A_A U_A = A_B U_B \quad (5)$$

But  $U_A = U_a$  and  $U_B = U_b$  and so equation 5 can be rewritten as

$$U_a = U_b A_B / A_A \quad (6)$$

Applying Bernoulli's equation between point "a" and "f" (along the stream line abf, Figure 2) gives:

$$U_a^2 / 2g + P_a / \rho g = U_f^2 / 2g + P_f / \rho g \quad (7)$$

$$\text{But } U_f = U_m$$

Substituting equation (6) into equation (7) and rearranging, we have:

$$(P_a - P_f) / \rho g = [U_m^2 - (A_B / A_A)^2 U_b^2] / 2g \quad (8)$$

Dividing both side of equation (8) by  $U_m^2$  we have:

$$(P_a - P_f) / (\rho U_m^2) = 0.5 - 0.5 (A_B / A_A) (U_b / U_m)^2 \quad (9)$$

$$\text{But } A_B / A_A = 0.183$$

and from tracer gas measurements,  $U_b/U_m = 0.916$

Substituting the values of  $A_B/A_A$  and  $U_b/U_m$  into equation (9), gives:

$$(P_a - P_f)/(\rho U_m^2) = 0.423 \quad (10)$$

Consider the variation of static pressure with  $X$ , Figure 3. The difference between the static pressure at  $X = 0$  (i.e. pressure  $\approx$  atmospheric pressure) and the static pressure of fully developed flow,  $X = L_e$  is given by:

$$h_a - h_x = (Z + Y) = Z + L_e \tan\theta \quad (11)$$

or

$$h_a - h_x = \rho_w g Z + dh_x/dx \quad (12)$$

For fully developed flow,  $h_x = -h_f$ . Multiplying both sides of equation (12) by  $\rho_w g$  we have:

$$P_a - P_f = \rho_w g Z + L_e dP/dx \quad (13)$$

From reference (9)

$$\tau_w = -D_H/4 (dP/dx) \quad (14)$$



Substituting equation (14) into (13) and dividing both side of equation (13) by  $\rho U_m^2$ , we have:

$$(P_a - P_f)/(\rho U_m^2) = \rho_w g Z/(\rho U_m^2) - 4 L_e \tau_w / (D_h \rho U_m^2) \quad (15)$$

From reference (9)

$$U_\tau = (\tau_w/\rho)^{0.5} \quad (16)$$

and

$$U_\tau = U_b (f/2)^{0.5} \quad (17)$$

Substituting equations (16) and (17) into equation (15) and simplifying, we have:

$$(P_a - P_f)/(\rho U_m^2) = \rho_w g Z/(\rho U_m^2) - 2 (L_e f/D_h) (U_b/U_m)^2 \quad (18)$$

From tracer gas measurements;  $U_b/U_m = 0.916$

and from reference (9)

$$f = 0.079 Re^{-0.25} \quad (19)$$

Substituting the value of  $U_b/U_m$  and equation (19) into (18) and simplifying, we have

$$(P_a - P_f)/(\rho U_m) = \rho_w g Z/(\rho U_m^2) - 0.1325 (L_e/D_h) Re^{-0.25} \quad (20)$$

Substituting equation (10) into (20) and simplifying we have:

$$L_e/D_h = [7.55 \rho_w g Z/(\rho U_m^2) - 3.19] Re^{0.25} \quad (21)$$

The intercepts,  $Z$ , of the static pressure lines were found from Figure 4. Figure 5 shows a plot of  $\rho_w g Z/\rho U_m^2$  versus  $Re$ . The best fit was used to determine the following equation:

$$\rho_w g Z/\rho U_m^2 = 0.5112 + 0.00003 Re \quad (22)$$

Substituting equation (22) into equation (21) we get:

$$L_e/D_h = (0.67 + 2.26 \times 10^{-4} Re) Re^{0.25} \quad (23)$$

This equation can be used to determine the entrance length,  $L_e$ , for fully developed turbulent flow.

## RESULTS AND DISCUSSION

The tracer gas constant injection method, a hot-wire anemometer and a pitot tube were used to measure turbulent air flow in the fully developed region of the duct (i.e,  $X/D_h = 105$ ). Figure 6 shows a comparison between measurements of duct air flow rates made using the tracer gas technique and measurements made using a hot-wire anemometer and a pitot tube. The tracer gas results were generally found to be in a good agreement with those obtained using the hot-wire and the pitot tube. However, there were uncertainties in the measurements as both the hot-wire and pitot tube are sensitive to alignment with the flow as

well as to turbulence level. The difficulty in measuring the velocity close to the duct wall and the internal cross-sectional area of the duct causes additional errors.

A further type of error arises owing to the use of an integration method (Simpson's rule) for estimating the flow rate in the duct. To reduce the error in the calculation, a large number of velocity measurements across the duct is required and the integration interval should be sufficiently small to allow the function to be well represented by line segments.

We also carried out measurement of centre line velocity along the length of the duct for various Reynolds numbers. The velocity was determined using the constant injection technique as well as the hot-wire anemometer and pitot tube. Figure 7 shows a typical variation of centre line velocity for different values of  $X/D_h$ . The tracer gas was injected at a position  $X/D_h = 21.9$  and the concentration in air was monitored at various positions downstream. Due to poor mixing of tracer gas close to the injection point, the estimated velocities were found to be less than those measured using the hot-wire and pitot tube. However, for fully developed flow the results were in closer agreement and the estimated velocities from the tracer gas measurements lay between those obtained using the hot-wire and the pitot tube.

The variation of tracer gas concentration along the length of the duct for various Reynolds numbers is shown in Figure 8. The concentration of tracer gas was found to decrease at the inlet of the duct as  $X/D_h$  increased. The concentration of tracer gas remained constant when the flow was fully developed. For low Re a large  $X/D_h$  was required for the concentration of tracer gas to reach a constant value.

Measurement of velocity (using a pitot tube) at various distances from the duct wall was also carried out. Turbulent velocity profiles for  $Re = 1.4 \times 10^4$  and different values of  $X/D_h$  are presented in Figure 9. It is apparent that the velocity profile changes shape from

one section to another in accordance with boundary layer development. For other Reynolds numbers, velocity profiles along the duct were found to behave in a similar manner.

The theoretical analysis to determine the entrance length required for fully developed flow shows that:

$$L_e/D_h = (0.67 + 2.26 \times 10^{-4} Re) Re^{0.25} \quad (\text{Equation 23})$$

From the pitot tube measurements of velocity distribution at various  $X/D_h$ , the following equation is obtained:

$$L_e/D_h = -2.276 + 0.00352 Re \quad (24)$$

The variation of  $L_e/D_h$  versus  $Re$  is shown in Figure 10. For turbulent flow with  $Re$  greater than 16000, an entrance length greater than 50 hydraulic diameter was necessary for the formation of a fully developed velocity profile. The entrance length predicted by the theoretical equation was found to be slightly less than that obtained from the pitot tube measurements. Equations 23 and 24 are only applicable to ducts of a similar type to the one used in our work as the formation of fully developed flow depends on factors such as the entrance configuration, the turbulence of the entering stream, the aspect ratio and the roughness of the duct.

## CONCLUSIONS

The use of the constant injection tracer gas technique was found to be a convenient means for measuring air flow in ducts. Estimated air flow derived from measurements made

using the tracer gas technique was found to be in good agreement with that obtained from measurements made using a hot wire anemometer and a pitot tube.

Tracer gas measurements were used to derive an equation describing the entrance length for fully developed flow. This was found to be in close agreement with the entrance length obtained from pitot tube measurements of the velocity profile at various  $X/D_h$ .

## REFERENCES

1. A.K.M.F. Hussain and W.C. Reynolds, "Measurements in fully developed turbulent channel flow", J Fluid Eng. Trans. ASME, Vol.97, pp.568-580, (1975).
2. T. Liou and J. Lin, "Measurement of turbulent flow in a duct with repeated ribs applied to opposite walls", J. Chinese Institute of Engineers, 11(4), pp.319-326, (1988).
3. J.P. Hartnett, J.C.Y. Koh and S.T. McComas, "A comparison of predicted and measured friction factors for turbulent flow through rectangular ducts", J of Heat and Mass Transfer, Trans. ASME, pp.82-88, (1962).
4. S.B. Riffat and M. Eid, "Measurement of air flow between the floors of houses using a portable SF<sub>6</sub> system", Energy and Building, 12(1), pp.67-75, (1988).
5. S.B. Riffat, "Interzone air movement and its effect on condensation in houses", Applied Energy, 32(1), pp.49-69, (1989).

6. L. Lagus and A.K. Persily, "A review of tracer-gas techniques for measuring airflows in buildings", ASHRAE Trans., Vol.91, Part 2B, HI-B5-22, No.1, pp.1075-1087, (1985).
7. L. Lundin, "Air leakage in industrial buildings-preliminary results", Proceedings of the 4th AIVC Conference "Air Infiltration Reduction in Existing Buildings", (Elm, Switzerland), pp.6.1-6.8, September (1983).
8. J. Axley and A. Persily, "Integral mass balances and pulse injection tracer gas techniques", Proceedings of the 9th AIVC Conference 'Effective Ventilation', (Gent, Belgium), paper no.7, September (1987).
9. V.L. Streeter and E.B. Wylie, "Fluid Mechanics", First SI Metric Edition, (McGraw-Hill International Book Company, Ltd), (1983).

## FIGURES

- Figure 1 Schematic diagram of the experimental system.
- Figure 2. Development of turbulent flow in a two-dimensional duct.
- Figure 3. Variation of static pressure with X.
- Figure 4. Static pressure distribution along the duct for various values of Re.
- Figure 5. Variation of  $\rho_w g Z/\rho U_m^2$  with Re.
- Figure 6. Comparison of tracer gas duct air flow measurements and measurements made using a hot-wire anemometer and a pitot tube.
- Figure 7. Variation of centre line velocity with  $X/D_h$ .
- Figure 8. Variation of tracer gas concentration with  $X/D_h$  for various values of Re.
- Figure 9. Turbulent velocity profiles at various distances from the duct entrance.
- Figure 10. Variation of  $L_e/D_h$  with Re.

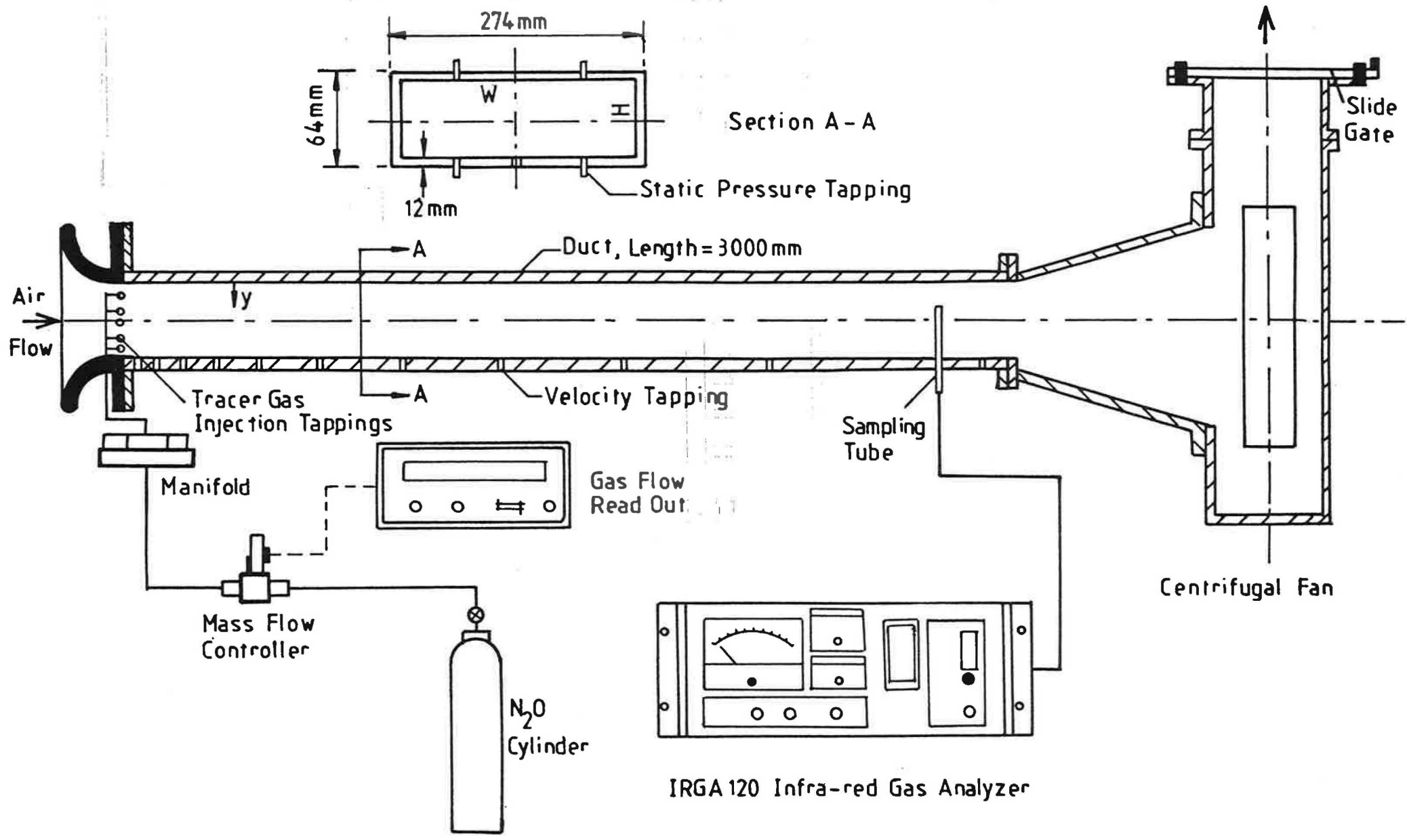


Fig.1



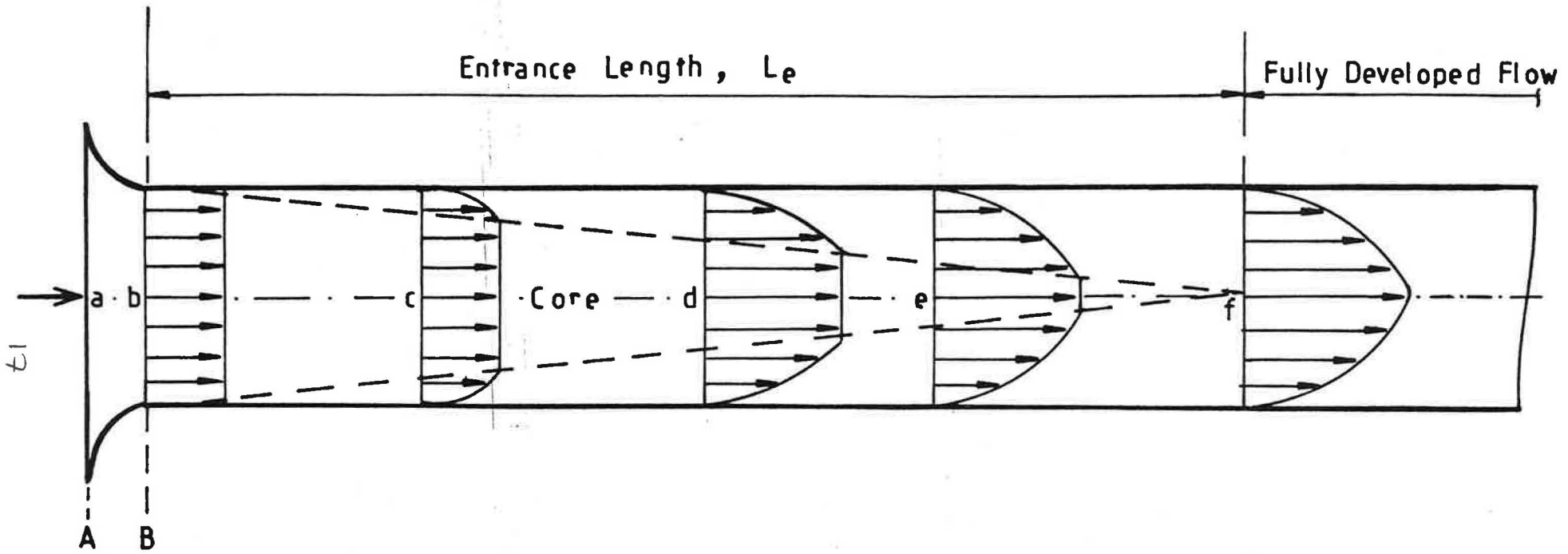


Fig. 2

18

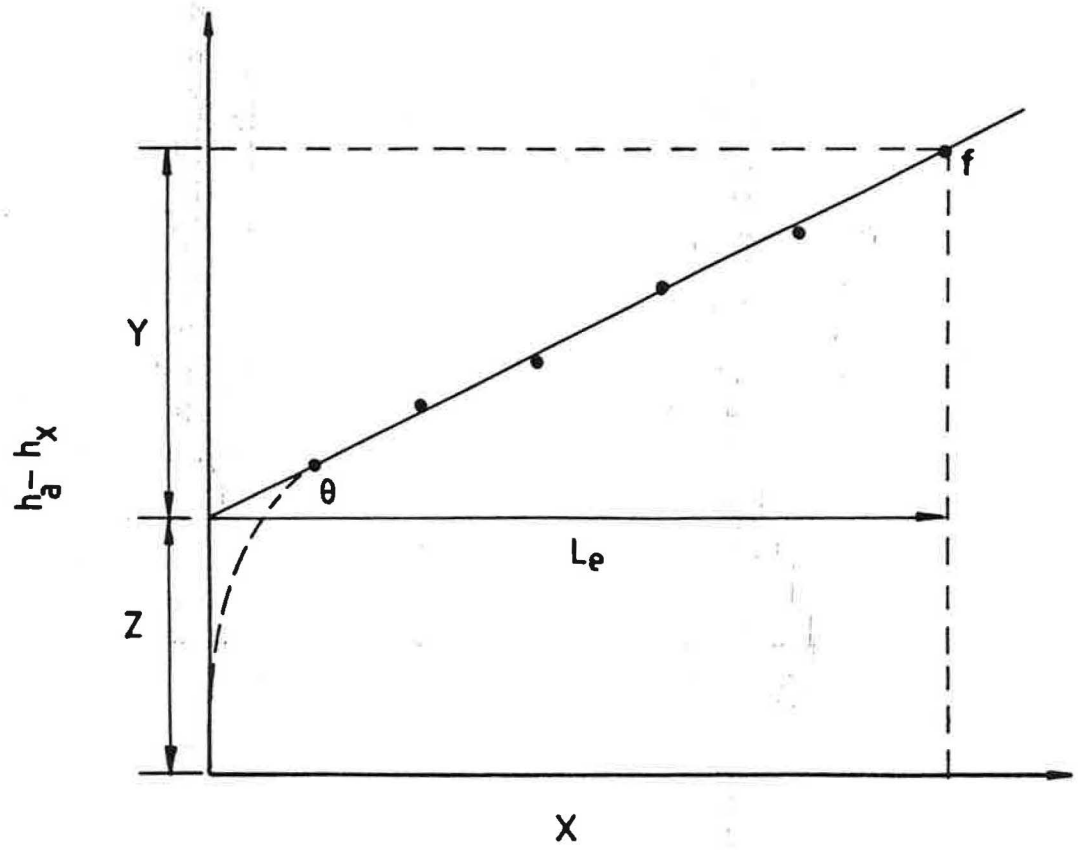


Fig. 3

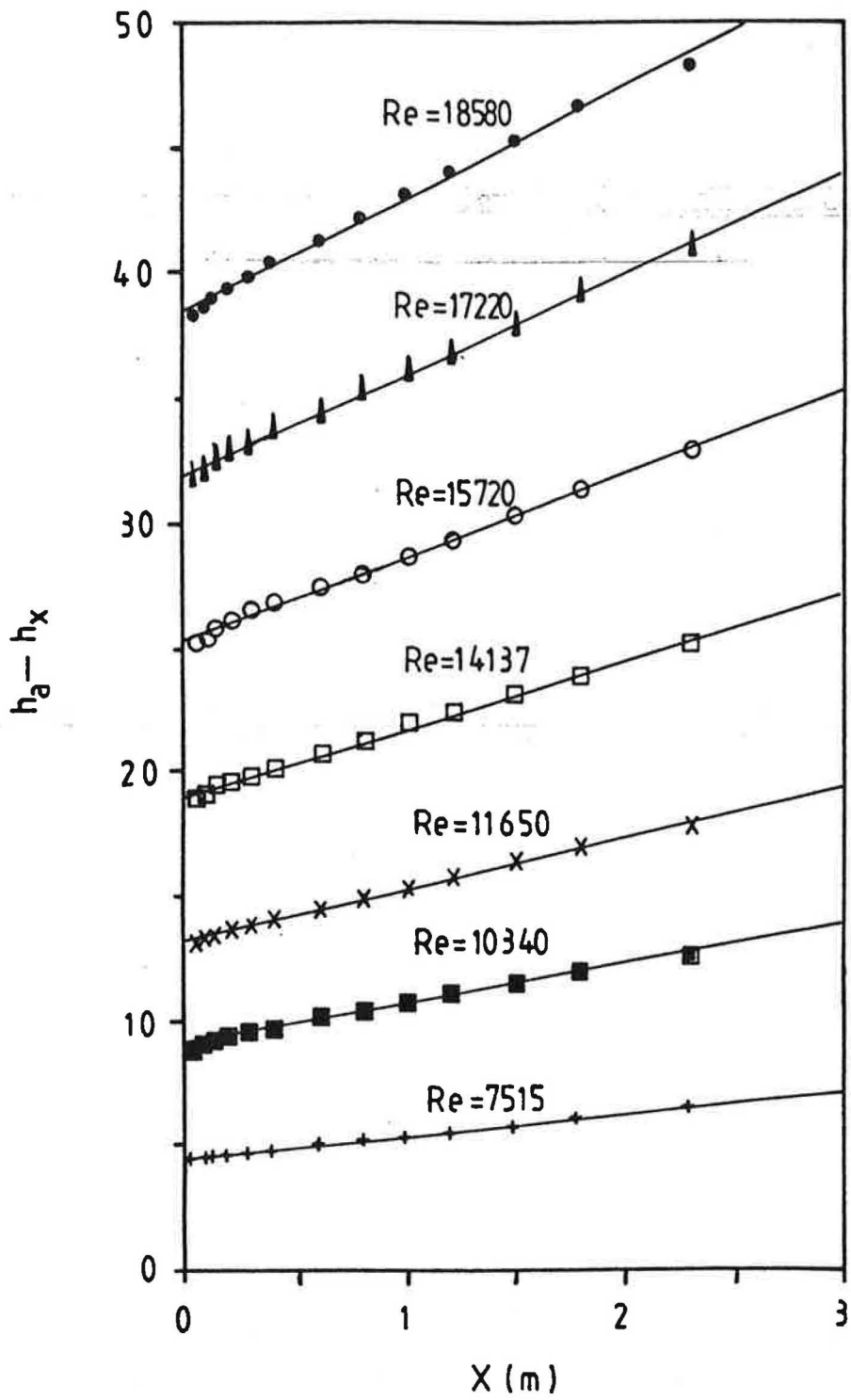


Fig.4

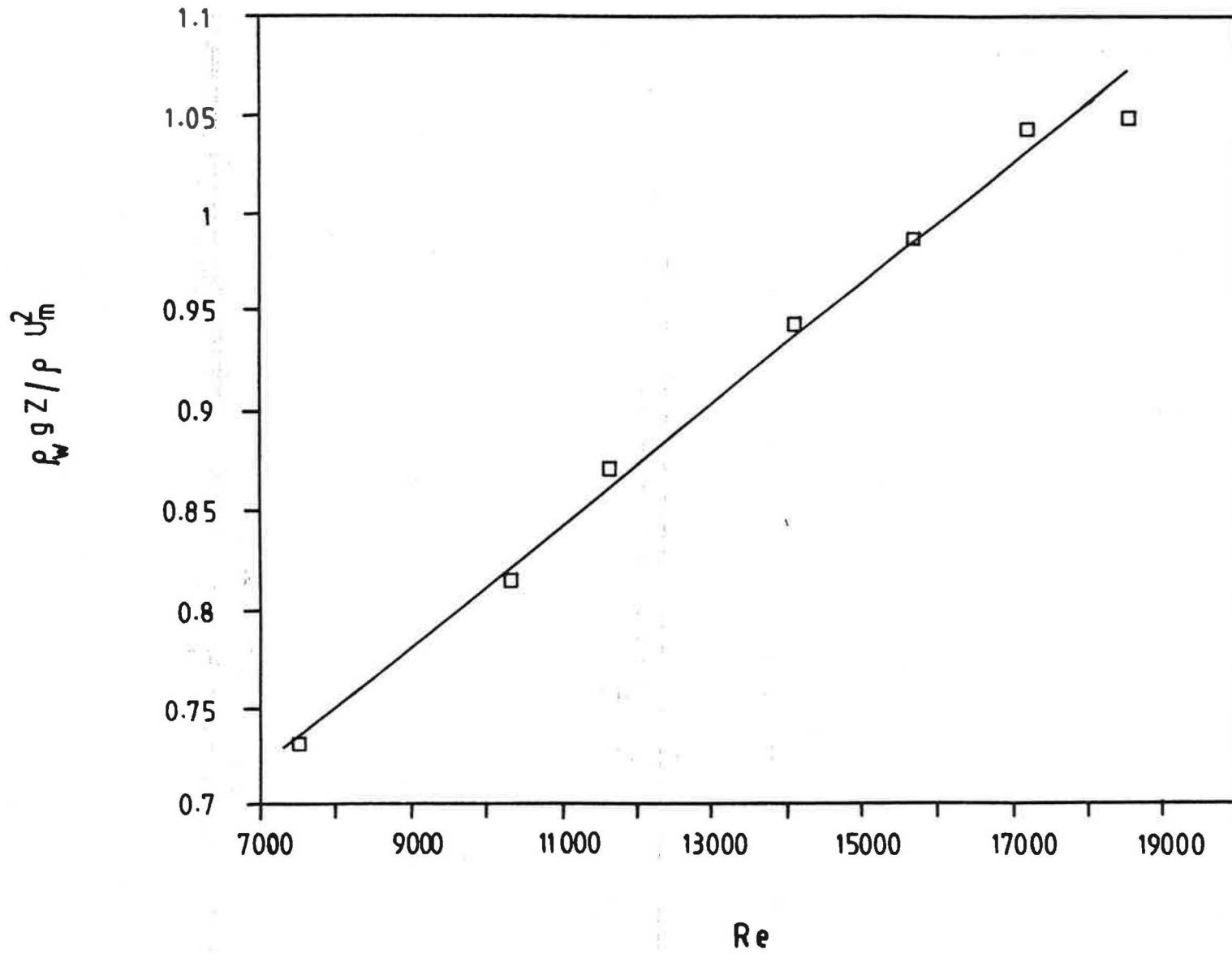


Fig.5

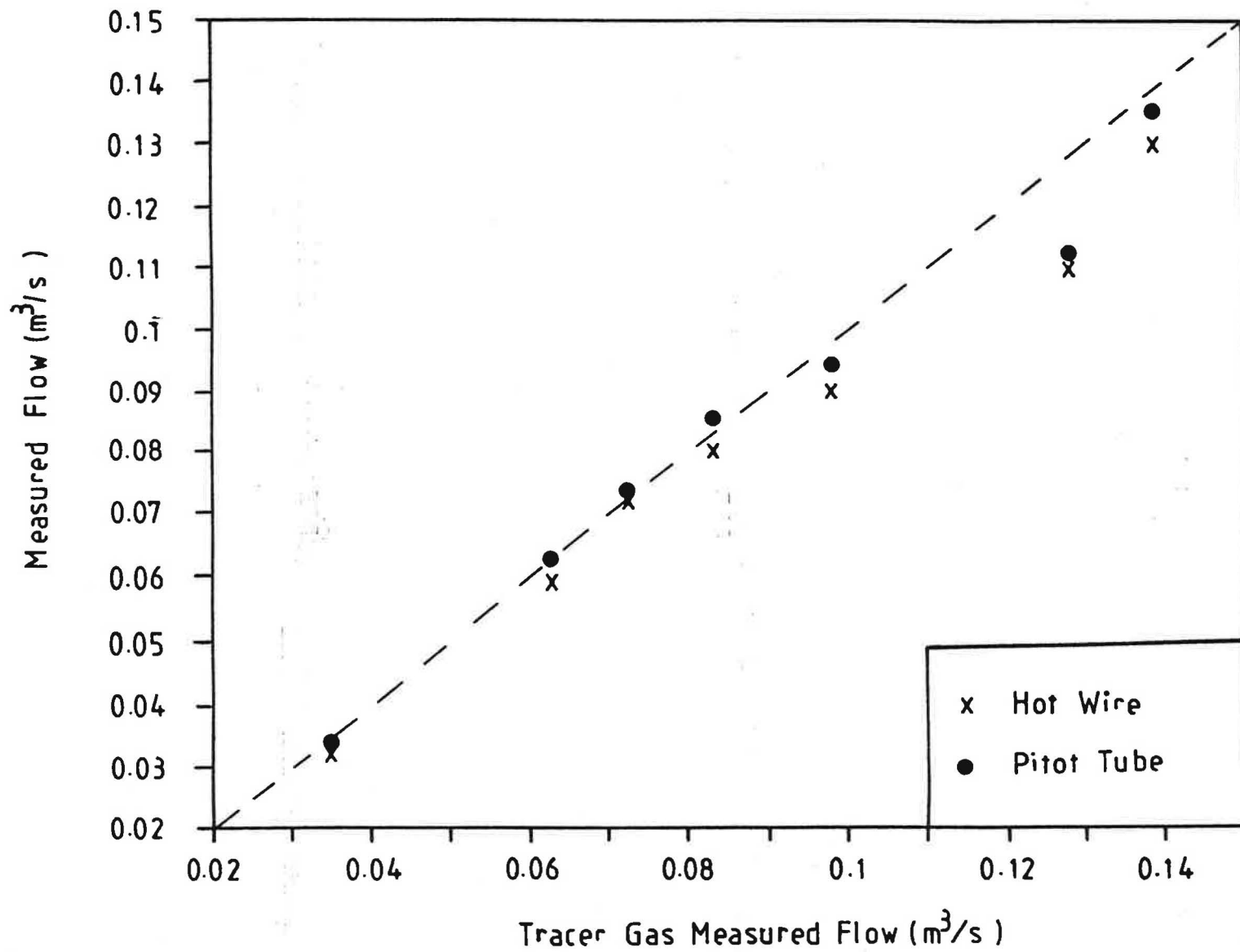


Fig.6

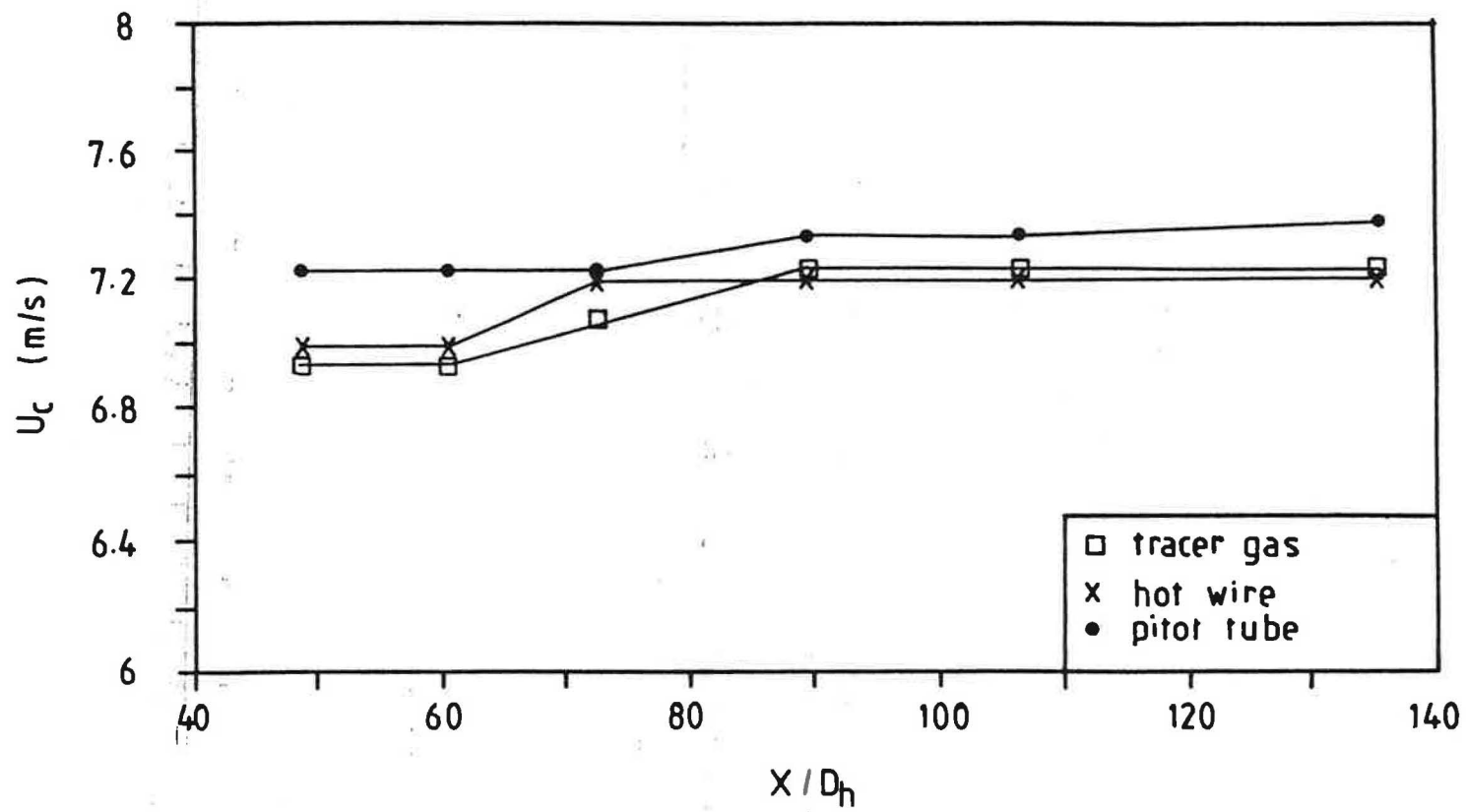


Fig.7

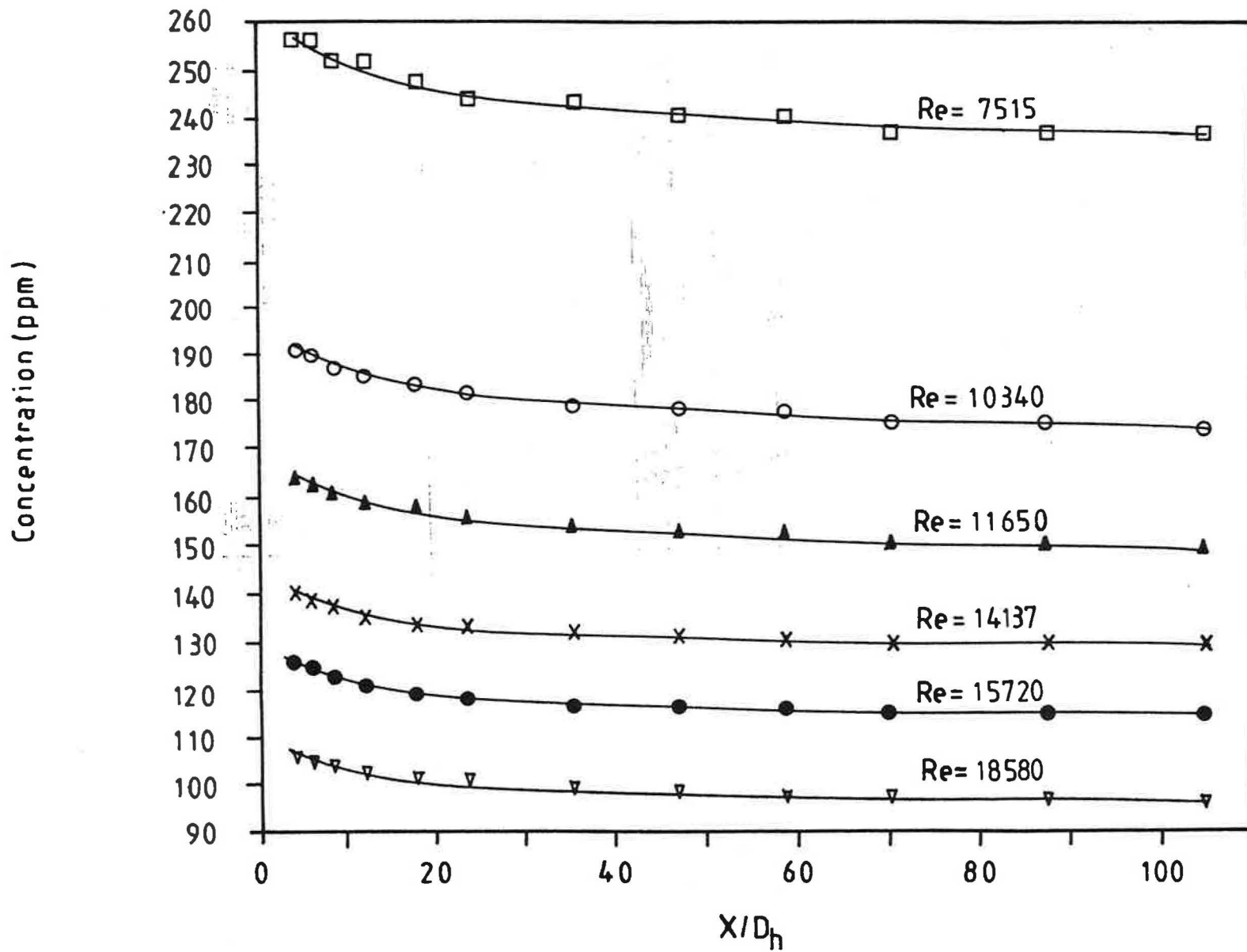


Fig. 8

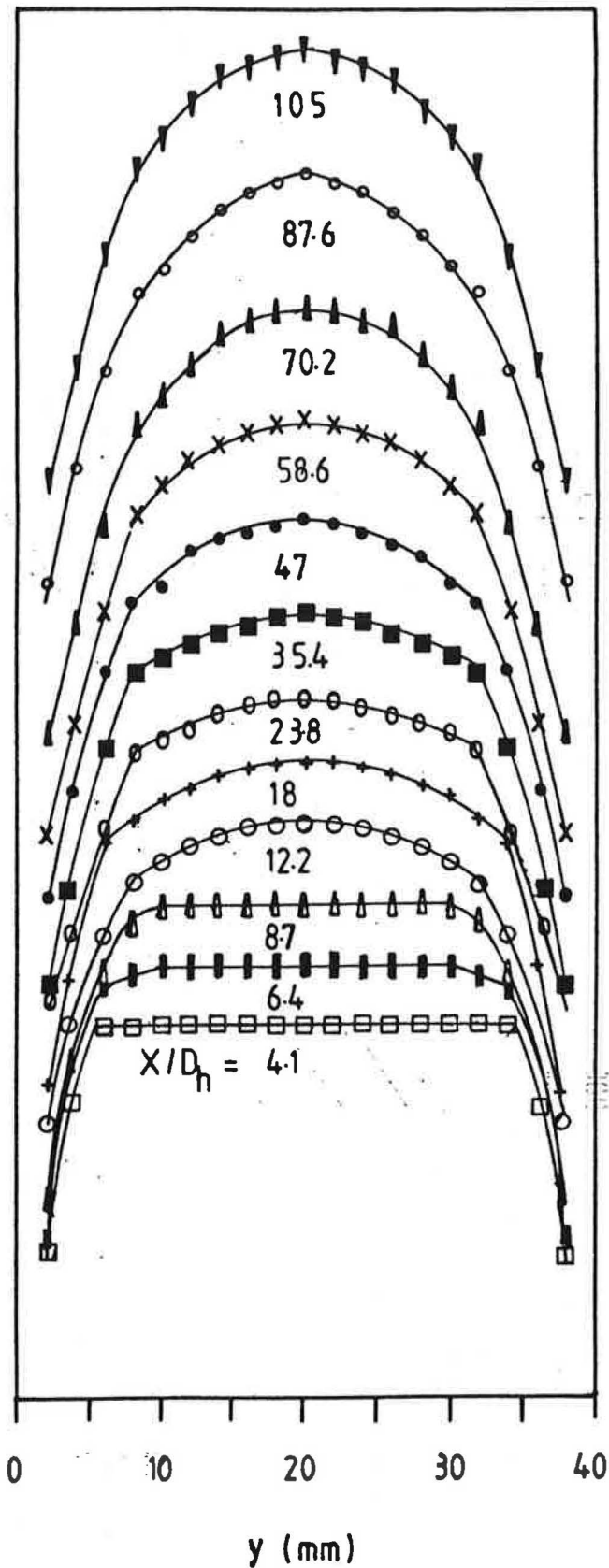


Fig. 9



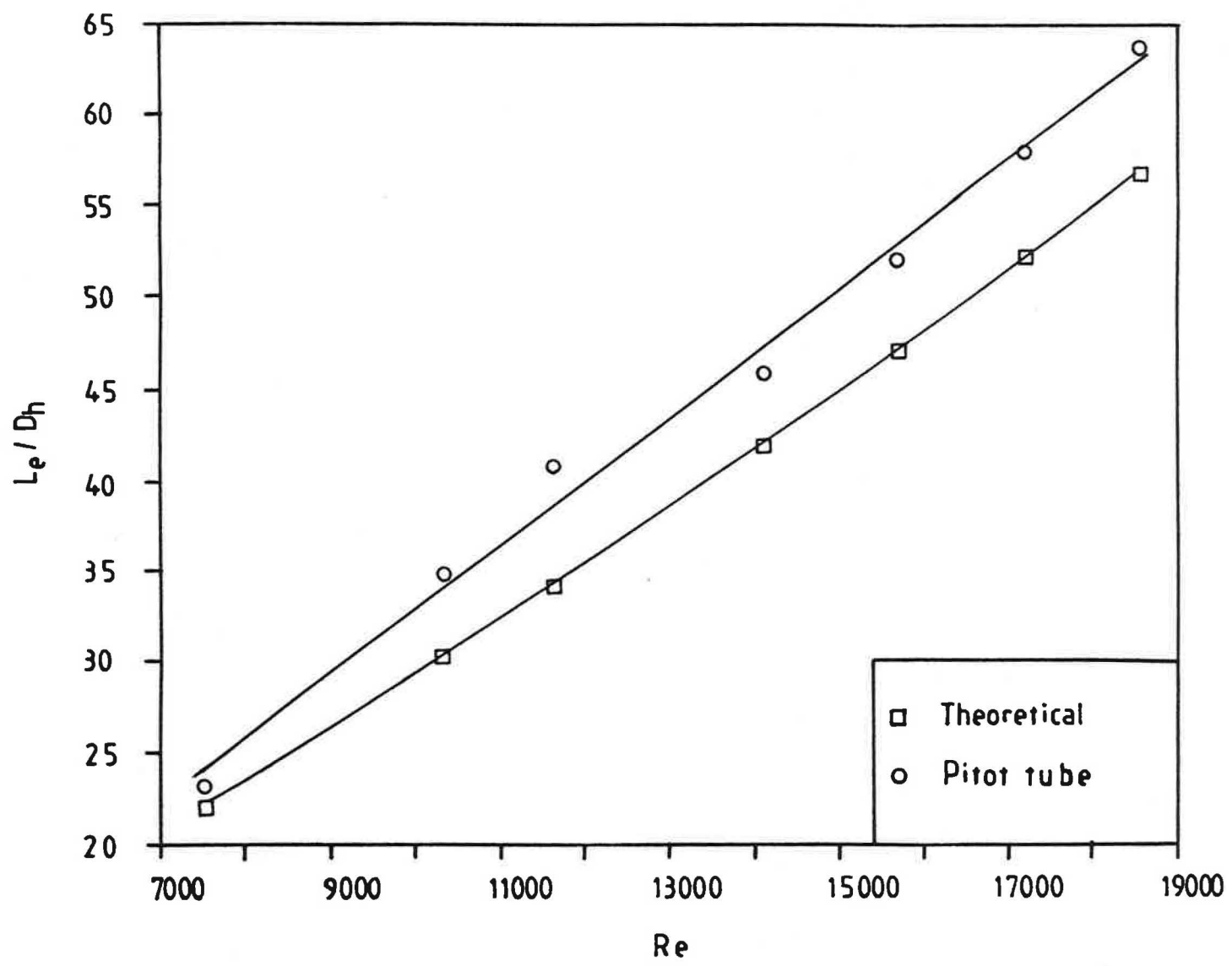


Fig.10